

## Field electron emission from polycrystalline GaN nanorods

S. Hasegawa\*, S. Nishida, T. Yamashita and H. Asahi

*The Institute of Scientific and Industrial Research, Osaka University, 8-1 Mihogaoka, Ibaraki, Osaka 567-0047, Japan*

We have grown polycrystalline GaN both on polycrystalline Mo sheets and on Si(001) substrates with native oxide by using plasma-assisted molecular beam epitaxy. It has been found that GaN growth on Si(001) with native oxide produces well *c*-orientated nanorods exhibiting a low field emission threshold of 1.25 V/ $\mu\text{m}$  at 0.1  $\mu\text{A}/\text{cm}^2$  and a high emission current density of 2.50 mA/ $\text{cm}^2$  at an applied electric field of 2.5 V/ $\mu\text{m}$ . We will review the growth of polycrystalline GaN films and the evaluation of their structural properties and electron field emission characteristics.

**Key words:** polycrystalline GaN, plasma-assisted MBE, field electron emission, nanorod.

### Introduction

Field electron emitters have attracted much attention since solid-state electron sources are one of the key devices for fabricating vacuum microelectronic devices and flat panel displays. Recent efforts have been devoted to studies on carbon nanotubes (CNTs) and ZnO-based nanostructures [1-5] along with improvements of conventional Spindt-type Mo field emitter arrays [6]. Since Mo, CNTs, and ZnO have work functions or electron affinities of around 4.5 eV, sharp tip-like or needle-like structures are required to obtain sufficient electron emission at low electric fields. On the other hand, since GaN has a low electron affinity of 2.7-3.3 eV in addition to strong chemical and mechanical stability, GaN has attracted considerable attention as a material for field emitters. We have reported that polycrystalline GaN grown on Mo by molecular beam epitaxy (MBE) exhibits good field emission characteristics due to a low electron affinity and their grain structures [7-10]. When compared with CNTs [1, 2] and ZnO-based nanostructures [3-5], the field enhancement factor is still low and the resultant turn-on electric field is high. To improve the field emission characteristics, we have grown GaN nanorod films on Si(100) with native oxide layers showing a sufficiently low turn-on electric field and a high emission current density. This paper will present our recent progress on the growth and the field emission properties of polycrystalline GaN for field electron emitter applications.

### Experimental Procedure

The GaN layers were grown by gas source MBE with

an ion removal electron cyclotron resonance (ECR) radical cell or a radio frequency (RF) nitrogen radical cell. The ECR radical cell has two magnets located in parallel at the exit of the ECR liner to remove ions with a removal efficiency of over 99% [11]. For the RF radical cell, an electric field was used to remove ions. Elemental Ga, and ECR or RF plasma-enhanced  $\text{N}_2$  were used as group III and group V sources, respectively. Substrates used were polycrystalline Mo sheets and Si(001) wafers with native oxides. Mechanically mirror-polished Mo surfaces were sequentially cleaned in hot baths of trichloroethylene, acetone, and alcohol. Then, the Mo surfaces were etched in an HCl solution for 20 minutes. The roughness of the Mo substrate surfaces was 1-2 nm root mean square (rms). Prior to GaN growth, substrates used in this study were thermally cleaned at 750-850 °C for 10-15 minutes without plasma-enhanced nitrogen irradiation in the gas source MBE growth chamber.

The growth conditions and procedure of GaN were the same as those used for the optimized growth of GaN on sapphire substrates [11]. Low-temperature- (LT-) GaN buffer layers (thickness: about 3 nm) were grown at 400 °C. On the LT-GaN buffer layers, GaN layers without intentional doping were grown at 650-830 °C with an  $\text{N}_2$  flow rate of 1.0-1.5 sccm and a Ga flux of  $1.3\text{-}4 \times 10^{-5}$  Pa. The growth rate was 0.1-0.3  $\mu\text{m}/\text{h}$ . Growth of GaN without the LT-GaN buffer layer was not conducted in this study.

Crystalline quality was determined by reflection high-energy electron diffraction (RHEED), X-ray diffraction (XRD) using Cu  $\text{K}\alpha$  radiation, scanning electron microscopy (SEM), and atomic force microscopy (AFM). Field emission (FE) measurements were carried out in an ultrahigh vacuum system with a base pressure of about  $10^{-7}$  Pa. The typical distance between the anode and the sample was 0.1 mm. The respective areas of the GaN/Mo and GaN/Si samples were  $1 \times 1 \text{ cm}^2$  and

\*Corresponding author:  
Tel : +81-6-6879-8407  
Fax: +81-6-6879-8409  
E-mail: hasegawa@sanken.osaka-u.ac.jp

$0.7 \times 0.7 \text{ cm}^2$ . The area of the anode was  $0.8 \times 0.8 \text{ cm}^2$ .

### Growth and Field Emission Properties of Polycrystalline GaN on Mo Substrates [7-9]

In the initial stage of GaN growth on Mo by using ECR plasma activated nitrogen, the growth of a LT-GaN buffer layer at  $400^\circ\text{C}$  generally precedes the growth of a desired layer. The LT-GaN buffer layer exhibited a ring RHEED pattern, indicating polycrystalline GaN growth without any preferential texture on polycrystalline Mo. During the growth of the desired layers at  $700\text{--}800^\circ\text{C}$ , the RHEED pattern gradually changed into a broken ring (arc) pattern shown in Fig. 1. This shows the formation of a preferential texture in the film. Figure 2 shows a typical perspective AFM image of the GaN surfaces grown on polycrystalline Mo substrates at  $700^\circ\text{C}$ . The average grain size and the surface roughness are  $400 \text{ nm}$  and  $64.8 \text{ nm rms}$ , respectively. The AFM image also shows that there are tip-like regions at the grains. These grain structures are expected

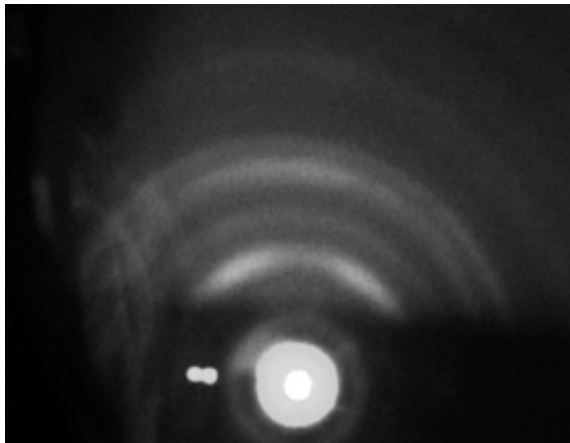


**Fig. 1.** RHEED pattern for a polycrystalline GaN film grown on Mo at  $700^\circ\text{C}$ .

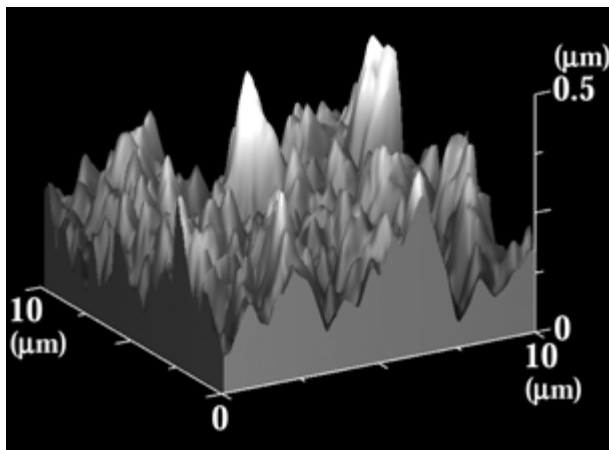


**Fig. 2.** Perspective AFM image ( $10 \mu\text{m} \times 10 \mu\text{m}$ ) for a polycrystalline GaN film grown on Mo at  $700^\circ\text{C}$ .

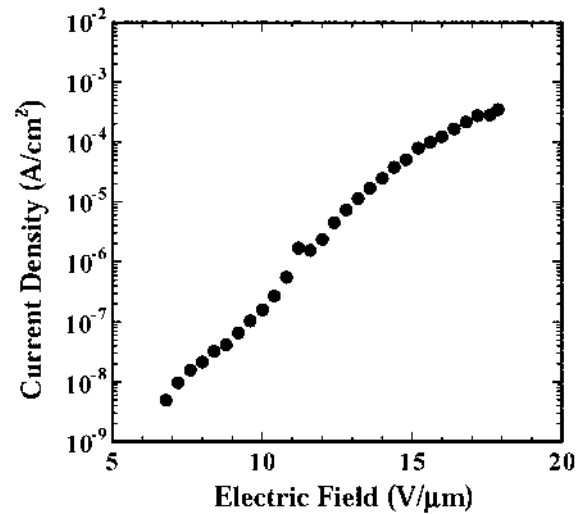


**Fig. 3.** Plot of the field emission current density versus applied electric field for a polycrystalline GaN film grown on Mo at  $700^\circ\text{C}$ . The distance between the GaN surface and the anode was  $0.1 \text{ mm}$ .

to lower a turn-on electric field for field emission.

Figure 3 shows a field emission current density versus applied electric field curve for the GaN/Mo sample grown at  $700^\circ\text{C}$ . The threshold field emission electric field is  $6.4 \text{ V}/\mu\text{m}$ , where the threshold electric field is designated as the electric field at an emission current of  $10 \text{ nA}/\text{cm}^2$ . We obtained a field emission current density of  $346 \mu\text{A}/\text{cm}^2$  at an electric field of  $18 \text{ V}/\mu\text{m}$ . GaN/Mo samples grown at other substrate temperatures ranging from  $650^\circ\text{C}$  to  $820^\circ\text{C}$  showed a larger threshold electric field and a lower field emission current density than those grown at  $700^\circ\text{C}$  [9]. The good field emission characteristics of the polycrystalline GaN films grown at  $700^\circ\text{C}$  are believed to be due to the tip-like structures observed in the AFM image. In order to produce efficient field emission of electrons, the field enhancement effect of tip-like structures is usually used. Actually, low threshold electric fields were obtained for some tip-like structures, which were formed by a growth technique and plasma treatment for BN [12], AlN [13] and GaN [14] systems.

Assuming an electron affinity of  $3.3 \text{ eV}$  [15, 16], the field enhancement factor  $\gamma$  is estimated from the linear portion of the Fowler-Nordheim (F-N) plot ( $J/F^2$ - $1/F$  relation) [17, 18]. F-N plots for the GaN/Mo film at  $700^\circ\text{C}$  are shown in Fig. 4. The straight line confirms electron emission due to the F-N tunneling mechanism. From the slope of the straight line, the field enhancement factor  $\gamma$  of the GaN/Mo film grown at  $700^\circ\text{C}$  is evaluated to be 280. For single-crystalline GaN,  $\gamma$  was reported to be 61 and 120 from the as-grown smooth surface and from the plasma-treated rough surface, respectively [14]. The as-grown GaN/Mo sample shows a large  $\gamma$  value because of the strong field enhancement due to the grain structures.

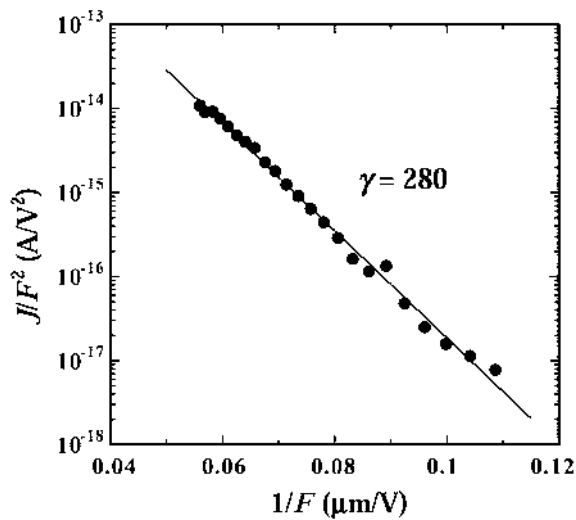


**Fig. 4.** Fowler-Nordheim plot for a polycrystalline GaN film grown at 700 °C.

### Growth and Field Emission Properties of GaN Nanorod Films on Si Substrates with Native Oxide [19]

Because of the low electron affinity and their grain structures, polycrystalline GaN films grown on polycrystalline Mo substrates at 700 °C showed good FE characteristics. In comparison with the FE characteristics reported on CNTs [1, 2] and ZnO-based nanostructures [3-5], the field enhancement factor was still low and the resultant turn-on electric field was high. In order to improve the field enhancement factor of polycrystalline GaN, we have grown polycrystalline GaN on Si(001) substrates with native silicon oxide by using RF plasma activated nitrogen. Since the polycrystalline GaN films grown on quartz (SiO<sub>2</sub>) consist of columns aligned along *c*-axis [11], it is expected that such GaN columns

aligned along the *c*-axis would be grown on Si with silicon oxide and have a large field enhancement factor.

Shown in Fig. 5 are RHEED patterns during the growth of GaN on Si(001) with native oxides. During the growth of LT-GaN layers at 400 °C, the surfaces exhibit only ring RHEED patterns, as shown in Fig. 5(a). This indicates polycrystalline GaN is grown on native oxide at 400 °C. As the LT-GaN layers are annealed at 680 °C without the irradiation by plasma-activated nitrogen, the ring pattern gradually changes into an arc RHEED pattern shown in Fig. 5(b). The appearance of the arc RHEED pattern is proof that a preferential texture is formed in the films. Analyzing the arc RHEED patterns in detail, it is found that annealing of the LT-GaN layers at 680 °C results in the nucleation of hexagonal GaN crystallites with their *c*-axis parallel to the substrate normal. GaN films grown at 680 °C on the annealed LT-GaN buffer layer show 3 dimensional (3D) transmission RHEED patterns, as shown in Fig. 5(c). When rotating the samples around the surface normal of the substrates, the same RHEED patterns were always observed. This indicates that the GaN layers consist of crystallites aligned along the *c*-axis without any in-plane preferential orientation. In other words, GaN layers with a (0001) fiber texture are grown on Si with native oxide.

Figure 6 shows a perspective AFM image of a polycrystalline GaN film grown on a Si(001) substrate with native oxide. It is found that GaN grains having almost the same diameter, around 80 nm, are uniformly distributed over the substrate. Moreover, the GaN films have quite rough surfaces and there are some grains which protrude substantially from the surface. From the RHEED and AFM results, it can be seen that the polycrystalline GaN films consist of single crystalline GaN nanorods with a diameter of around 80 nm. Figure 7 shows a cross-sectional transmission electron microscopy (XTEM) image taken from a GaN film grown on a Si

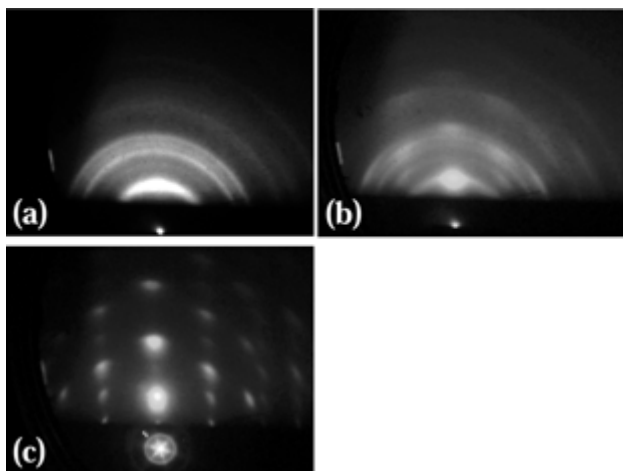


**Fig. 5.** RHEED patterns (a) after growth of LT-GaN at 400 °C, (b) during annealing of LT-GaN at 680 °C, (c) after growth of GaN at 680 °C.

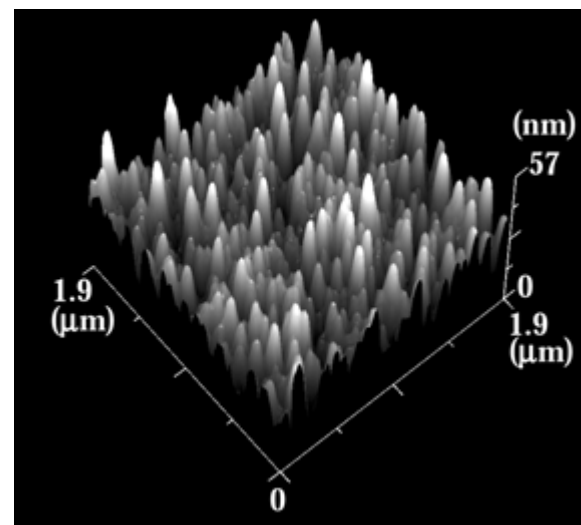


**Fig. 6.** Perspective AFM image (1.92 μm × 1.92 μm) for a GaN/SiO<sub>2</sub>/Si sample.

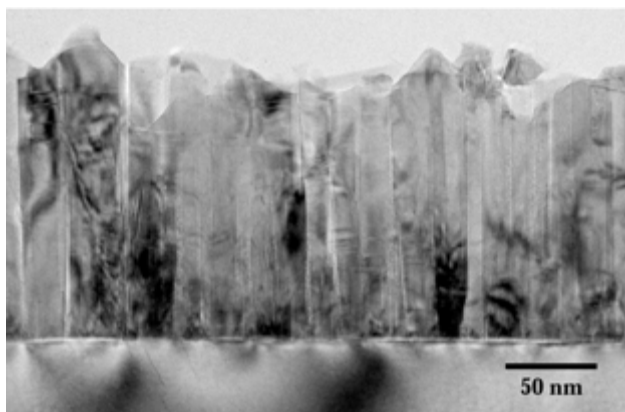


Fig. 7. XTEM image for a GaN/SiO<sub>2</sub>/Si sample.

(001) substrate with native oxide. This provides clear evidence that single crystalline GaN nanorods grow on the substrate. Moreover, we noticed that some nanorods protruding from the surface have sharp tip-like configurations. Such sharp tips on top of nanorods are expected to sufficiently lower the turn-on electric field for field emission.

Figure 8(a) shows an emission current density versus electric field curve acquired from the GaN nanorod films. It can be seen that the GaN nanorod films exhibit excellent field emission characteristics with a threshold emission field of 1.25 V/ $\mu$ m at a current density of 0.1  $\mu$ A/cm<sup>2</sup> and a field emission current density of 2.50 mA/cm<sup>2</sup> at an applied electric field of 2.5 V/ $\mu$ m. The excellent FE characteristic is attributed to the large field enhancement at the tips of nanorods as well as a low electron affinity of GaN. The Fowler-Nordheim (F-N) plot ( $J/F^2$ - $1/F$  relation) is shown in Fig. 8(b). A straight line indicates that the electron emission is due to the F-N tunneling mechanism. From the slope of the straight line, the field enhancement factor  $\gamma$  is calculated to be 1270 in the low electric field region. Clearly, the GaN nanorod film exhibits a much larger  $\gamma$  value than the polycrystalline GaN grown on Mo because of the strong local electric field enhancement resulting from the geometrical configurations. The field enhancement factor of 1270 is somewhat smaller than those of CNTs (1000-50000) [1, 2], tetrapot-like ZnO nanostructures (6285) [3], and ZnO nanofibers (2991) [5]. Since GaN has much a lower electron affinity than CNTs and ZnO, the turn-on electric field of GaN nanorods is quite low (1.25 V/ $\mu$ m at 0.1  $\mu$ A/cm<sup>2</sup>) as compared with CNTs (0.6-0.8 V/ $\mu$ m) [2], tetrapot-like ZnO nanostructures (1.6 V/ $\mu$ m at 1.0  $\mu$ A/cm<sup>2</sup>) [3], and ZnO nanofibers (2.4 V/ $\mu$ m at 0.1  $\mu$ A/cm<sup>2</sup>) [5].

## Conclusions

We have grown polycrystalline GaN films both on polycrystalline Mo sheets and on Si(001) substrates with native silicon oxide. Polycrystalline GaN films on

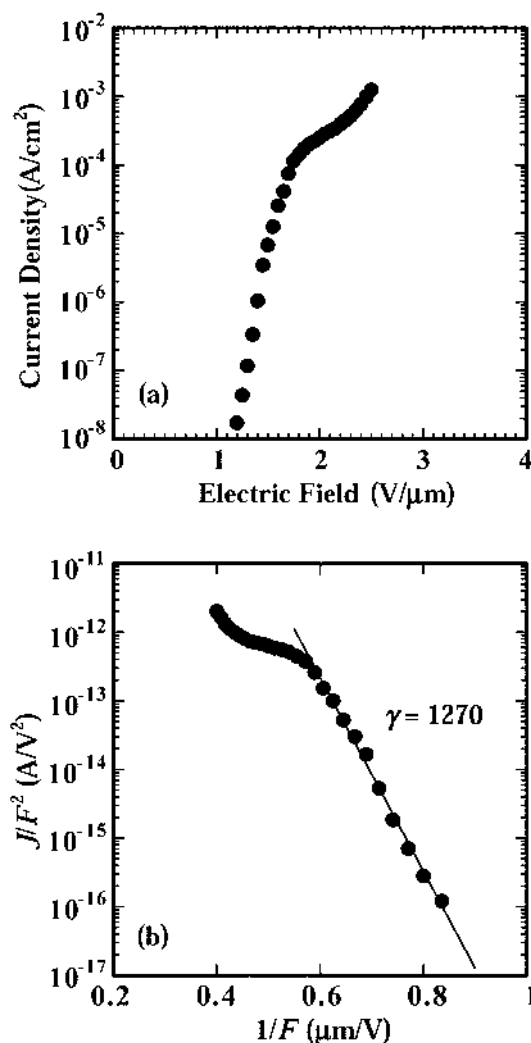


Fig. 8. (a) Plot of the electron emission current density versus applied electric field for a GaN/SiO<sub>2</sub>/Si sample and (b) the corresponding Fowler-Nordheim plot.

mechanically polished Mo substrates showed good field emission characteristics due to the grain structures and the low electron affinity of GaN. To improve the field emission characteristics of the polycrystalline GaN films, GaN nanorod films have been grown on Si(001) substrates with native oxide. The resultant GaN nanorod films exhibited a low field emission threshold of 1.25 V/ $\mu$ m at 0.1  $\mu$ A/cm<sup>2</sup> and a high field emission current density of 2.50 mA/cm<sup>2</sup> at an applied electric field of 2.5 V/ $\mu$ m. The structural and electrical properties of polycrystalline GaN provide that polycrystalline GaN is one of the promising materials for field electron emission devices.

## Acknowledgement

This work was supported in part by the Grant-in-Aid for Scientific Research (B) from the Ministry of Education, Culture, Sports, Science and Technology (MEXT) of Japan.

## References

1. J.M. Bonard, J.P. Salvetat, T. Stockli, W.A. de Heer, L. Forro, and A. Chatelain, *Appl. Phys. Lett.* 73 (1998) 918-920.
2. S.C. Kung, K.C. Hwang, and I.N. Lin, *Appl. Phys. Lett.* 80 (2002) 4819-4821.
3. Q. Wan, K. Yu, T.H. Wang, and C.L. Lin, *Appl. Phys. Lett.* 83 (2003) 2253-2255.
4. C.X. Xu and X.W. Sun, *Appl. Phys. Lett.* 83 (2003) 3806-3808.
5. C.X. Xu, X.W. Sun, and B.J. Chen, *Appl. Phys. Lett.* 84 (2004) 1540-1542.
6. S. Itoh, M. Tanaka, and T. Toneyawa, *J. Vac. Sci. Technol. B* 22 (2004) 1362-1366.
7. H. Tampo, T. Yamanaka, K. Yamada, K. Ohnishi, M. Hashimoto, and H. Asahi, *Jpn. J. Appl. Phys.* 41 (2002) L907-L909.
8. T. Yamanaka, H. Tampo, K. Yamada, K. Ohnishi, M. Hashimoto, and H. Asahi, *Phys. Stat. Sol. (c)* 0[1] (2002) 469-473.
9. S. Nishida, T. Yamanaka, S. Hasegawa, and H. Asahi, *Phys. Stat. Sol. (c)* 0[7] (2002) 2416-2419.
10. S. Nishida, T. Yamashita, S. Hasegawa, and H. Asahi, *Thin Solid Films* 464-465 (2004) 128-130.
11. K. Iwata, H. Asahi, S.-J. Yu, K. Asami, H. Fujita, M. Fushida, and S. Gonda, *Jpn. J. Appl. Phys.* 35 (1996) L289-L292.
12. T. Sugino, Y. Etou, S. Tagawa, M.N. Gamo, and T. Ando, *J. Vac. Sci. Technol. B* 18, (2000) 1089-1092.
13. M. Kasu and N. Kobayashi, *Appl. Phys. Lett.* 78 (2001) 1835-1837.
14. T. Sugino, T. Hori, C. Kimura, and T. Yamamoto, *Appl. Phys. Lett.* 78 (2001) 3229-3231.
15. O.H. Nam, M.D. Michael, D. Bremser, B.L. Ward, R.J. Nemanich, and R.F. Davis, *Jpn. J. Appl. Phys.* 36 (1997) L532-L535.
16. C.I. Wu and A. Khan, *J. Appl. Phys.* 86 (1999) 3209-3212.
17. R.H. Fowler and L.W. Nordheim, *Proc. R. Soc. London, Ser. A* 119 (1928) 173-181.
18. R. Gomer, in "Field Emission and Field Ionization" (American Institute of Physics, 1993) p. 9.
19. T. Yamashita, S. Hasegawa, S. Nishida, M. Ishimaru, Y. Hirotsu, and H. Asahi, *Appl. Phys. Lett.* 86 (2005) 082109-1-082109-3.